

**U-Load
Dextramer®**

Build multimers with your choice of peptide and peptide-receptive MHC I and MHC II alleles.



Blockade of Antimicrobial Proteins S100A8 and S100A9 Inhibits Phagocyte Migration to the Alveoli in Streptococcal Pneumonia

This information is current as of February 24, 2022.

Marie-Astrid Raquil, Nadia Anceriz, Pascal Rouleau and Philippe A. Tessier

J Immunol 2008; 180:3366-3374; ;
doi: 10.4049/jimmunol.180.5.3366
<http://www.jimmunol.org/content/180/5/3366>

References This article **cites 48 articles**, 22 of which you can access for free at:
<http://www.jimmunol.org/content/180/5/3366.full#ref-list-1>

Why *The JI*? [Submit online.](#)

- **Rapid Reviews! 30 days*** from submission to initial decision
- **No Triage!** Every submission reviewed by practicing scientists
- **Fast Publication!** 4 weeks from acceptance to publication

**average*

Subscription Information about subscribing to *The Journal of Immunology* is online at:
<http://jimmunol.org/subscription>

Permissions Submit copyright permission requests at:
<http://www.aai.org/About/Publications/JI/copyright.html>

Email Alerts Receive free email-alerts when new articles cite this article. Sign up at:
<http://jimmunol.org/alerts>



Blockade of Antimicrobial Proteins S100A8 and S100A9 Inhibits Phagocyte Migration to the Alveoli in Streptococcal Pneumonia¹

Marie-Astrid Raquil, Nadia Anceriz, Pascal Rouleau, and Philippe A. Tessier²

We investigated the roles of the potent, chemotactic antimicrobial proteins S100A8, S100A9, and S100A8/A9 in leukocyte migration in a model of streptococcal pneumonia. We first observed differential secretion of S100A8, S100A9, and S100A8/A9 that preceded neutrophil recruitment. This is partially explained by the expression of S100A8 and S100A9 proteins by pneumocytes in the early phase of *Streptococcus pneumoniae* infection. Pretreatment of mice with anti-S100A8 and anti-S100A9 Abs, alone or in combination had no effect on bacterial load or mice survival, but caused neutrophil and macrophage recruitment to the alveoli to diminish by 70 and 80%, respectively, without modifying leukocyte blood count, transendothelial migration or neutrophil sequestration in the lung vasculature. These decreases were also associated with a 68% increase of phagocyte accumulation in lung tissue and increased expression of the chemokines CXCL1, CXCL2, and CCL2 in lung tissues and bronchoalveolar lavages. These results show that S100A8 and S100A9 play an important role in leukocyte migration and strongly suggest their involvement in the transepithelial migration of macrophages and neutrophils. They also indicate the importance of antimicrobial proteins, as opposed to classical chemotactic factors such as chemokines, in regulating innate immune responses in the lung. *The Journal of Immunology*, 2008, 180: 3366–3374.

In recent years, the differences between antimicrobial peptides and chemotactic factors have become less distinct. For example, some CC and CXC chemokines such as CCL20 and CXCL10 have been reported to inhibit microbial growth (1, 2). Conversely, defensins, cathepsin G, and CAP37/azurocidin, which are well known for their antimicrobial properties, have recently been shown to be chemotactic for T lymphocytes, monocytes, and neutrophils (3–5). S100A8 and S100A9 are other antimicrobial proteins that exert characteristic chemotactic and proinflammatory activities.

S100A8 and S100A9 are expressed by neutrophils, monocytes, and activated endothelial and epithelial cells (6–10). They exist as noncovalently bound homodimers, but also as heterodimers (S100A8/A9) that inhibit bacterial adhesion to mucosal epithelium and bacterial growth through zinc chelation (10–20). Studies on inflammatory disorders such as cystic fibrosis, gout, and rheumatoid arthritis have shed light upon the association between the secretion of these S100 proteins in biological liquids and pathogenesis (8, 21–25).

In addition to their antimicrobial properties, S100A8, S100A9, and S100A8/A9 are potentially chemotactic for neutrophils and monocytes (26, 27). These proteins are involved in transendothelial migration of leukocytes by inducing neutrophil adhesion to fibrinogen by activation of the β_2 integrin Mac-1 (26, 28). They

also participate in neutrophil migration to inflammatory sites in response to LPS and monosodium urate crystals (27, 29), which places them in the innate immune response.

Multiple chemotactic and antimicrobial factors are simultaneously present at the site of infection during the immune response; thus, the task of distinguishing their relative roles is rather complicated. In this study, we have further delineated the roles of S100A8 and S100A9 in leukocyte migration by studying bacterial load, leukocyte influx in the lung, and mouse survival that occurs in streptococcal pneumonia. Infection by *Streptococcus pneumoniae*, a major etiological agent of community-acquired pneumonia, which is the most common cause worldwide of death from infection (30), first takes hold through adhesion of these bacteria to the epithelium within the alveoli. This in turn causes local release of proinflammatory mediators such as cytokines, chemokines, and leukotrienes, which activate the surrounding tissue and further induce inflammatory factors in that tissue. Neutrophils and monocytes/macrophages are among the first cells to migrate to these sites of inflammation where they kill pathogens by phagocytosis, release of oxygen radicals and tissue degrading enzymes, or secretion of antimicrobial peptides.

We report here that S100A8 and S100A9 were released at high levels during the course of infection and that their presence correlated with increased neutrophil migration. More importantly, blockade of S100A8 and S100A9 activity was also associated with an accumulation of neutrophils and monocytes in lung tissue, exemplifying the importance of these antimicrobial proteins in regulating the migration of these cells to the lung alveoli more precisely in the epithelial migration.

Materials and Methods

S. pneumoniae infection

S. pneumoniae serotype 3 (isolated clinical strain) was grown in 100 ml of brain-heart infusion medium (Difco) at 37°C in 5% CO₂ to the midexponential phase (0.4 OD₆₀₀). Forty milliliters of bacteria culture were pelleted, washed twice, and resuspended in 10 ml of cold endotoxin-free PBS.

Centre de Recherche en Infectiologie, Centre de Recherche du Centre Hospitalier de l'Université Laval, and Faculty of Medicine, Laval University, Quebec, Canada

Received for publication November 29, 2006. Accepted for publication December 28, 2007.

The costs of publication of this article were defrayed in part by the payment of page charges. This article must therefore be hereby marked *advertisement* in accordance with 18 U.S.C. Section 1734 solely to indicate this fact.

¹ This work was supported by Canadian Institutes of Health Research Grant 57777 and the Fonds de la Recherche en Santé du Québec (to P.A.T.).

² Address correspondence and reprint requests to Dr. Philippe A. Tessier, Room RC 709, Centre de Recherche du Centre Hospitalier de l'Université Laval, 2705 Boulevard Laurier, Sainte-Foy, Quebec, Canada G1V 4G2. E-mail address: Philippe.Tessier@crchul.ulaval.ca

Copyright © 2008 by The American Association of Immunologists, Inc. 0022-1767/08/\$2.00

An OD at 600 nm was read, and an adequate dilution was made to obtain an inoculum of 4×10^5 CFU/50 μ l. The bacterial concentration was confirmed by serial dilutions of the inoculum plated on blood-agar. Female CD1 mice, 6–8 wk old (Charles River) were lightly anesthetized by isoflurane and intranasally instilled with 4×10^5 CFU of *S. pneumoniae* or endotoxin-free PBS. In some experiments, mice were injected i.p. 16 h before infection with 2 mg of purified neutralizing rabbit IgG anti-S100A8 and/or anti-S100A9, or with nonspecific rabbit IgG (27). At various times postinfection, the mice were sacrificed by carbon dioxide asphyxiation, and bronchoalveolar lavage (BAL)³ and lungs were collected as described (31). For survival studies, the morbidity and mortality of infected mice were carefully observed for up to 6 days. Bacterial clearance in anti-S100A8- and/or anti-S100A9-treated mice was determined by serial dilution of BAL and lung homogenates on blood-agar. Animal studies have been reviewed and approved by the Laval University animal protection committee.

Analyses of leukocyte recruitment and quantification of S100A8 and S100A9

BAL was centrifuged at 1200 rpm for 10 min, and the pelleted cells were resuspended in 600 μ l of PBS. Total leukocytes were stained with acetic blue and counted with a hemacytometer. Leukocyte subpopulations were determined by Wright-Giemsa stainings of cytopins. Lungs were homogenized in 2 ml of 50 mM phosphate buffer, pH 6, and then diluted by addition of an equal volume of 50 mM phosphate buffer, pH 6, containing 1% hexadecyltrimethylammonium bromide. Diluted homogenates were sonicated for 30 s and centrifuged at $3000 \times g$ for 30 min. The supernatants were used to evaluate neutrophil recruitment in the tissue by measuring endogenous myeloperoxidase. Briefly, in a 96-well plates, 15 μ l of myeloperoxidase standards (Sigma-Aldrich), and samples were mixed with 100 μ l of the reaction solution containing 0.01 mg/ml *o*-dianisidine and 0.004% H_2O_2 in phosphate buffer. After 10 min, 100 μ l of 1% sodium azide were added to stop the reaction (31). The OD was read at 450 nm. Quantification of S100A8, S100A9, and S100A8/A9 was done using by ELISA as previously described (27).

Immunohistochemistry, immunofluorescence, and electron microscopy

Lungs were perfused with 4% paraformaldehyde in PBS, fixed for 48 h at 4°C, dehydrated, and embedded in paraffin. For immunohistochemical detection of murine S100A8 and S100A9, 5- μ m tissue sections were rehydrated by serial immersion in 100% toluene; then 100, 95, 70, and 50% ethanol; and rinsed in PBS. After inhibition of endogenous peroxidase with 3% H_2O_2 in PBS for 20 min, nonspecific binding sites were blocked with 10% normal donkey serum (Sigma-Aldrich), 2% BSA in PBS. After three washings with PBS, tissue sections were incubated for 1 h at room temperature with purified anti-murine S100A8 or S100A9 rabbit polyclonal IgG Abs (10 μ g/ml) diluted in PBS, 2% normal donkey serum, 2% BSA. Tissue sections were rinsed three times with PBS and incubated for 1 h at room temperature with peroxidase-conjugated donkey anti-rabbit IgG (100 μ g/ml). After a washing, the peroxidase activity was revealed with a 3,3'-diaminobenzidine tetrahydrochloride (Sigma-Aldrich), 0.024% H_2O_2 solution for 5 min. Tissue sections were counterstained with H&E.

For immunofluorescence, paraffin-embedded lung sections were rehydrated and immersed for 1 h in 0.025% NH_3 , 70% ethanol to decrease autofluorescence. Lung sections were then blocked for 2 h in PBS, 10% normal goat serum (Sigma-Aldrich), 2% BSA, 0.2% Triton before being incubated overnight with a mix of 1/1000 rabbit anti-human prosurfactant protein C (proSP-C; Chemicon) and 1 μ g/ml rat anti-S100A8 or rat anti-S100A9 in PBS, 2% normal goat serum, 2% BSA. Equal amounts of isotype control IgG and purified preimmune serum were used as control. After six washes, tissue sections were incubated for 1 h with a mix of ALEXA-488-conjugated goat anti-rabbit IgG (1/200), ALEXA-555-conjugated goat anti-rat IgG (1/200), and the nuclear marker TOPRO-3 (1 μ M). Fluorescence was then examined using an Olympus Fluoview FV300 confocal microscope.

For electron microscopy analyses, lungs were fixed in 2.5% glutaraldehyde in phosphate buffer and post fixed in 1% osmium tetroxide. They were embedded in Epon and sectioned for transmission electron microscopy. The samples were then analyzed using a JEOL JEM-1230 transmission electron microscope at 80 kV.

Evaluation of neutrophils sequestration in the lung tissue using flow cytometry

The number of sequestered neutrophil following *S. pneumoniae* infection was measured following a variant of a protocol described in Ref. 32. Briefly, at 48 h postinfection, mice were injected i.v. with 10 μ g of FITC-labeled anti-Gr1 (to label sequestered neutrophils; Leinco Technologies) or FITC-labeled isotype control (IgG2b; Ebioscience). Ten minutes after injection, the mice were sacrificed by carbon dioxide asphyxia, and the blood, lungs, and BAL were harvested. The lungs were minced and digested using a solution of dispase 2.4 U/ml (BD Biosciences) and collagenase, 124 U/ml (Sigma-Aldrich), in the presence of excess unlabeled anti-Gr1 (to prevent labeling of transendothelial migrated neutrophils by residual labeled anti-Gr1; Leinco Technologies) or isotype control in PBS for 60–90 min at 37°C. After digestion, the lungs were passed through a 70- μ m cell strainer (BD Biosciences), centrifuged, and resuspended at 10×10^6 cells/ml in PBS, 2% FBS.

Separate aliquots of 1×10^6 cells from the blood, BAL, and lung were first incubated for 30 min with 0.5 μ g of murine Fc block (Ebioscience) in PBS-2% FBS (Wisent) to block Fc receptors. After three washes, the cells were incubated with 1 μ g of PE-labeled anti-7/4 (1/50) (to label all neutrophils; Serotec) or PE-labeled IgG2a (Ebioscience) for 30 min. After incubation, the cells were washed three times and fixed with PBS, 2% formaldehyde. Flow cytometry analysis was done on an EPICS XL Coulter flow cytometer. Sequestered neutrophils were determined by defining the Gr-1⁺ cells present in the 7/4⁺ (total neutrophil) population per million of 7/4⁺ cells (lung cells).

CXCL2, CXCL1, and CCL2 ELISA

For determination of CXCL2, CXCL1, and CCL2 protein levels, 96-well microtiter plates (NUNC) were coated overnight with goat Abs against CCL2, CXCL2, or CXCL1 in 0.1 M $NaHCO_3$, pH 9.6. The plates were washed three times with PBS, 0.05% Tween 20 (PBST) and blocked for 2 h with PBST, 2% BSA. Murine recombinant chemokine standards or the samples diluted in PBST, 2% BSA were then added and incubated for 2 h. After washing, biotinylated goat anti-CCL2, CXCL1, or CXCL2 were added for 1 h. Poly-HRP streptavidin (1/10,000) (Pierce Biotechnology) was incubated for 45 min, and the plates were revealed with 3,3',5,5'-tetramethylbenzidine substrate. The reaction was stopped with 0.18 N H_2SO_4 . The OD was read at 450 nm. The lower limit of quantification of these assays was 10 pg/ml. All Abs and recombinant murine chemokines were purchased from R & D Systems.

Statistical analysis

Experimental data are expressed as mean \pm SEM. One-way ANOVA with Dunnett's post test was performed using GraphPad InStat version 3.05 for Windows (GraphPad Software). Differences were considered statistically significant when $p \leq 0.05$.

Results

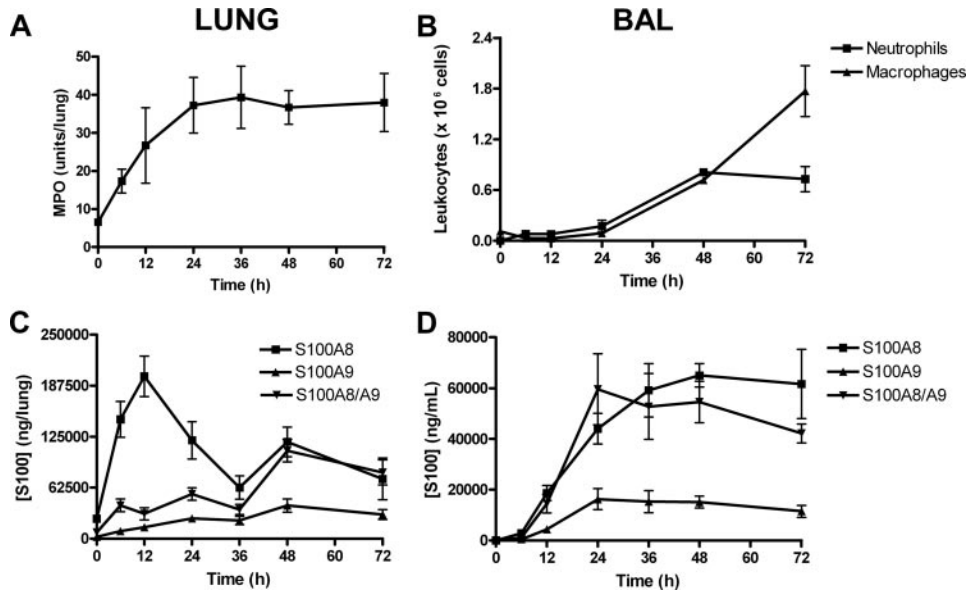
Secretion of S100A8 and S100A8/A9 precedes leukocyte recruitment during *S. pneumoniae* infection

To study the involvement of S100A8 and S100A9 in leukocyte recruitment, we used a murine model of *S. pneumoniae* lung infection. Mice were inoculated by nasal instillation with 4×10^5 CFU of *S. pneumoniae* to mimic the human infection. Lung infection was validated by the observation of progressive neutrophil and macrophage recruitment to the lung tissue and airspace. Neutrophil recruitment in lung tissue was first detected at 6 h, peaked by 24 h (Fig. 1A), and then remained constant until the death of the mouse. In contrast, neutrophil accumulation in the alveolar space was slower, with maximal infiltration of neutrophils ($\sim 8 \times 10^5$ cells) occurring at 48 h. Macrophage migration steadily increased during the infection, reaching a maximum of 1.8×10^6 cells at 72 h (Fig. 1B).

To determine the role of S100A8 and S100A9 in leukocyte migration during infection in the lungs, S100A8, S100A9, and S100A8/A9 were quantified in lung tissue and BAL of mice infected with *S. pneumoniae*. As shown in Fig. 1C, S100A8 rapidly peaked in lung tissue at close to 200 μ g/lung, appearing at 12 h before declining by 36 h postinjection. S100A8 preceded S100A9 and S100A8/A9 release, with maximum presence of these proteins detected at 48 h at ~ 40 and 107 μ g/lung, respectively. In contrast,

³ Abbreviations used in this paper: BAL, bronchoalveolar lavage; PBST, PBS 0.05% Tween 20.

FIGURE 1. Leukocyte recruitment and secretion of S100A8, S100A9, and S100A8/A9 in the lung and BAL after *S. pneumoniae* infection. CD1 mice were intranasally instilled with *S. pneumoniae*. At various times postinfection, lungs and BALs were collected. Recruited leukocytes were counted by measuring the myeloperoxidase in lung homogenates (A) and using a hemacytometer in BALs (B). The concentration of S100A8, S100A9, and S100A8/A9 was measured by ELISA in lung homogenates (C) and in the BALs (D). Data represent the mean \pm SEM of ≥ 6 mice per group.



concentrations of S100A8/A9 and S100A8 in the BAL peaked at 24 and 36 h (70 μ g/ml, both) and remained relatively constant until the death of the mouse (Fig. 1D). Interestingly, compared with the

other S100 proteins, little S100A9 was released in these conditions. Thus secretion of S100 proteins preceded infiltration of neutrophils in the lung and alveolar space. Moreover, the differential

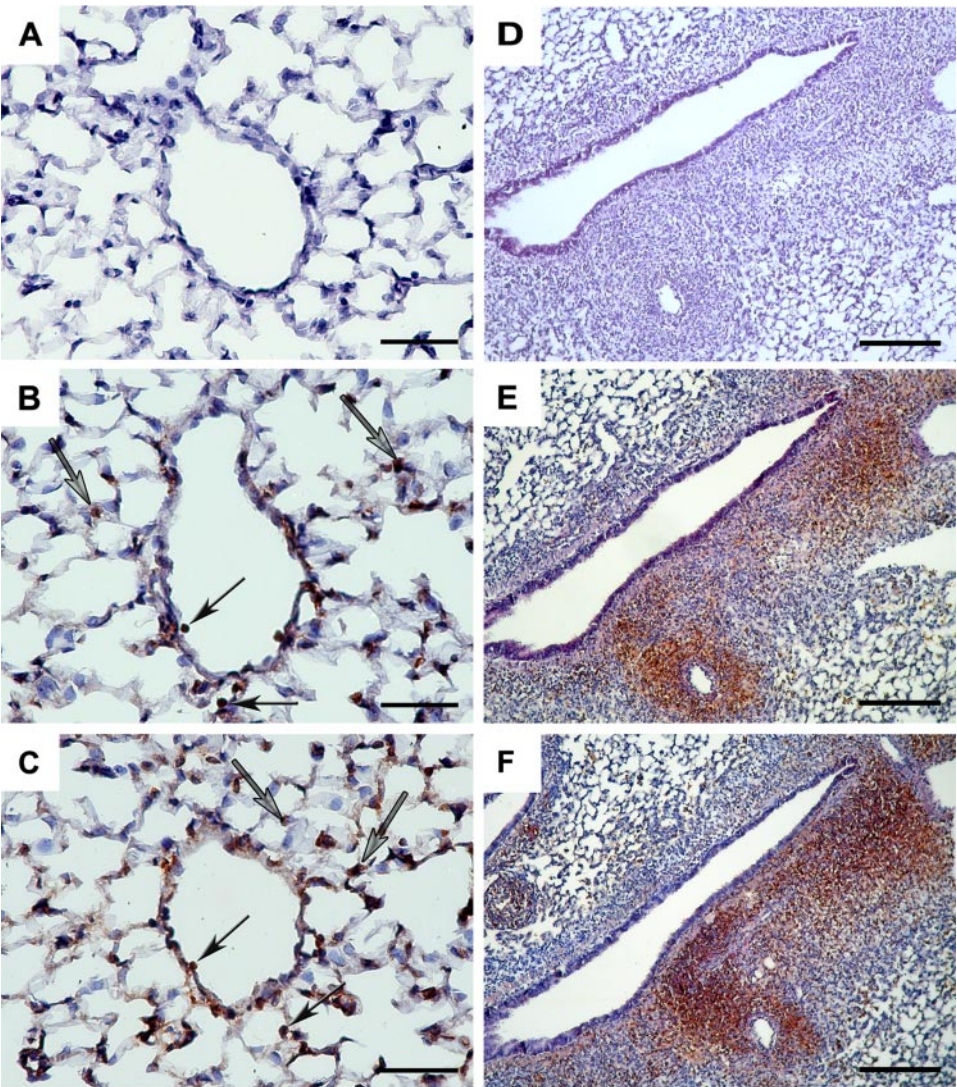


FIGURE 2. Localization of S100A8 and S100A9 at 6 and 48 h postinfection in *S. pneumoniae*-infected lung. CD1 mice were intranasally instilled with *S. pneumoniae*. Lungs were collected, washed, fixed in 4% paraformaldehyde, and embedded in paraffin. Lung sections 5 μ m thick, taken at 6 h (A–C) and 48 h (D–F) postinfection were incubated with rabbit anti-S100A8 (B and E, respectively), rabbit anti-S100A9 (C and F) or with preimmune IgGs (A and D). After washings, the sections were incubated with HRP-conjugated goat anti-rabbit, revealed with DAB substrate and counterstained with H&E. Scale bars in A–C correspond to 50 μ m, and those in D–F correspond to 200 μ m. A–C, $\times 400$; D–F, $\times 100$. Black and gray arrows point to the positive-staining pneumocytes and neutrophils, respectively.

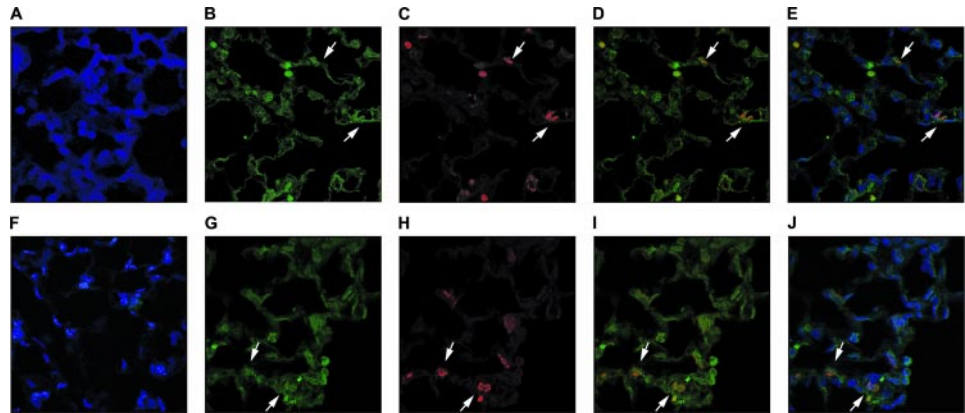


FIGURE 3. Localization of S100A8 and S100A9 in lung epithelial cells at 6 h postinfection by immunofluorescence. CD1 mice were intranasally instilled with *S. pneumoniae*. At 6 h postinfection, lung were harvested, fixed, and embedded in paraffin. Lung sections of 5 μ m were incubated with rabbit anti-proSP-C, rat anti-S100A8, or anti-S100A9, followed with a mix of Alexa488-labeled goat anti-rabbit, Alexa555-labeled goat anti-rat, and TOPRO-3. A and F, merged images of TOPRO-3 (blue) staining, rabbit preimmune serum (red) and IgG 2a or IgG1 κ as isotype control of rat anti-S100A8 and rat anti-S100A9 (green), respectively. B and G, S100A8 or S100A9 staining, respectively. C and H, pro-SPC staining. D and I, merged images of ProSP-C (red), and S100A8 or S100A9 (green), respectively. E and J, merged images of Topro-3 (blue), ProSP-C (red), and S100A8 or S100A9 (green), respectively. A–J, 900 \times magnification of areas close to neutrophil infiltration. Arrows represent double-positive staining of proSP-C and S100 proteins in type II pneumocytes (II).

release of these proteins suggested distinct roles for these proteins in the host primary responses to *S. pneumoniae*.

To further characterize the release of S100 proteins, we examined the localization of these proteins in the lung during infection. Immunostaining of lung tissue sections showed that S100A8 and S100A9 proteins were localized mainly in pneumocytes, neutrophils, and macrophages at early stages of infection (Fig. 2, A–C). Confocal imaging of lung tissue sections indicated that type II pneumocytes (proSPC⁺) expressed S100A8 and S100A9 (Fig. 3). Neutrophils and macrophages (data not shown) were also strongly positive for S100A8 and S100A9 proteins.

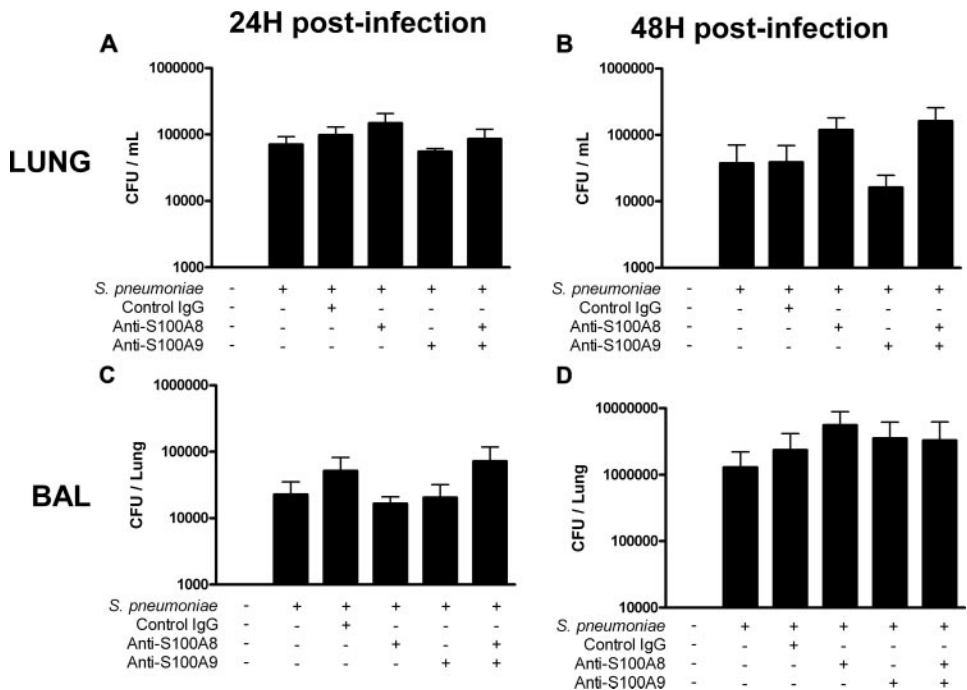
At later times postinfection, the lung tissue did not show diffused distribution of S100 proteins but rather defined localization around the inflamed bronchi and bronchioli. Their high levels at the inflammatory site were associated with a loss of integrity of the

leukocyte-infiltrated lung (Fig. 2, D–F). These results suggested that the antimicrobial proteins S100A8 and S100A9 could play important but distinct roles in the pathogenesis of *S. pneumoniae* infection.

Blockade of S100A8 and S100A9 activities significantly inhibits neutrophil and macrophage recruitment in the airspace

S100 proteins have both intracellular and extracellular activities. Conclusions from studies using knockout mice defective in S100A8 or S100A9 gene are therefore difficult to reach, as both intra- and extracellular activities are inhibited in these animals. In addition, S100A8-deficient mice die during embryogenesis (33). It is thus almost impossible to use knockout mice for the study of the extracellular activities of S100A8 and S100A9. To circumvent this problem, we used blocking mAbs to determine the importance of

FIGURE 4. Effects of S100A8 and S100A9 blockade on *S. pneumoniae* clearance at 24 and 48 h postinfection. CD1 mice were injected i.p. with 2 mg of rabbit anti-S100A8, anti-S100A9, or preimmune IgGs 16 h before being intranasally instilled with *S. pneumoniae*. At 24 and 48 h, BAL and lung were harvested, and serial dilutions of lung homogenates (A and B) and BAL (C and D) were plated in blood agar overnight at 37°C.



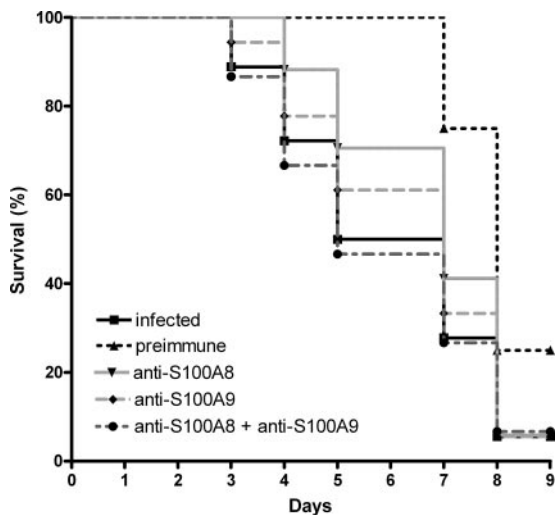


FIGURE 5. Effects of anti-S100A8 and anti-S100A9 on survival rates. CD1 mice were injected i.p. with 2 mg of rabbit anti-S100A8, anti-S100A9, or preimmune IgGs 16 h before being intranasally instilled with *S. pneumoniae*. Mortality was observed every 12 h for up to 9 days.

extracellular S100A8/A9 in leukocyte migration and disease genesis (27, 29). To examine the roles of S100A8 and S100A9 in innate immune responses to *S. pneumoniae*, their activities were blocked by i.p. injection of purified IgG directed against S100A8 and/or S100A9 16 h before infection. Interestingly, no significant changes were observed in *S. pneumoniae* clearance (Fig. 4) or the survival rates between treated and untreated infected mice (Fig. 5). Anti-S100A8 and anti-S100A9 slightly increased mouse survival rates (but not significantly), whereas the combination of both Abs had no effect. As expected, passive immunization with nonspecific Abs (preimmune serum) protected mice from early death associated with pneumonia (34).

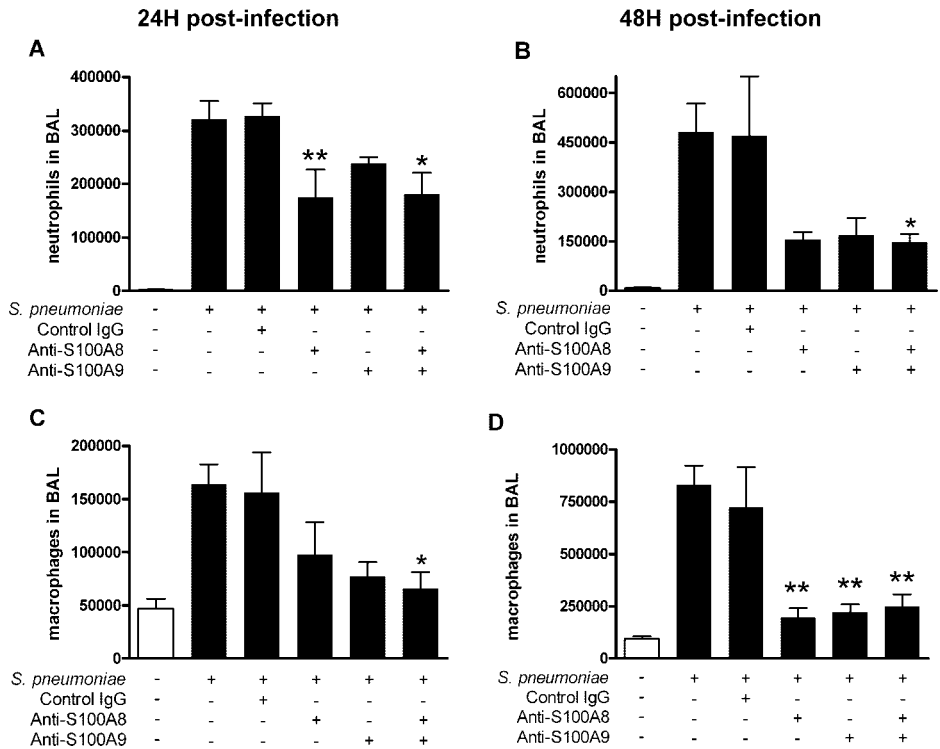
However, as seen in Fig. 6A, blockade of S100A8 and S100A9 activities led to a 45% decrease of neutrophils recruitment in the

BAL 24 h postinfection ($p < 0.01$ and $p < 0.05$ compared with control mice, Dunnett multiple comparison test). Moreover, at 48 h postinfection, pretreatment with anti-S100A8 and anti-S100A9 inhibited neutrophil migration to the alveolar space by 70% (Fig. 6B; $p < 0.05$, Dunnett multiple comparison test). These results indicated that S100A8 and S100A9 are required for neutrophil recruitment in the alveolar space. This requirement was even more important for macrophage recruitment, with a reduction of 82% in mice treated with anti-S100A8 and anti-S100A9 24 h postinfection (Fig. 6C; $p < 0.05$, Dunnett multiple comparison test). This result was confirmed at 48 h postinfection, where the blockade of S100A8 and S100A9, alone or in combination, led to a reduction of ~80% of macrophage infiltration in the alveolar space (Fig. 6D; $p < 0.01$, Dunnett multiple comparison test). These results indicated that S100A8 and S100A9 play an important role in the migration of leukocytes, and particularly macrophages, in the alveolar space during *S. pneumoniae* infection.

To determine at which stage of this migration cascade S100 proteins played a role, phagocyte migration to the lung tissue was evaluated by measuring endogenous myeloperoxidase. At 48 h postinfection, pretreating infected mice with anti-S100A8 and anti-S100A9 led to a 68% increase of endogenous myeloperoxidase in the lung tissue compared with the control mice (Fig. 7; $p < 0.05$, Dunnett multiple comparison test). This accumulation was associated with a decrease in leukocytes in the airspace, suggesting that S100A8 and S100A9 play a role in the transmigration of phagocytes from the lung tissue to the alveolar space.

To test this hypothesis, FITC-labeled anti-Gr1 (anti-neutrophil) Abs were injected i.v. 10 min before the mice were euthanized to stain sequestered neutrophils. The lungs were then harvested and single cell suspensions were analyzed by flow cytometry following labeling of all neutrophils with the neutrophil-specific Ab 7/4. Under these conditions, sequestered neutrophils were positively labeled with both FITC-labeled Gr1 and PE-labeled 7/4, whereas neutrophils that have already migrated in the tissue were labeled only with the Ab 7/4. As shown in Fig. 8A, the number of neutrophils present in the lung remained unchanged in anti-S100A8

FIGURE 6. Effects of S100A8 and S100A9 blockade on the recruitment of leukocytes in the BAL. CD1 mice were injected i.p. with 2 mg of purified rabbit IgG against S100A8, and/or S100A9, or nonimmune serum, 16 h before infection. Mice were then infected with *S. pneumoniae*. At 24 and 48 h postinfection, the BAL was collected. Recruited neutrophils (A and B) and macrophages (C, D) were counted using a hemacytometer at 24 h (A and C) and 48 h (B and D) postinfection. Values represent the mean \pm SEM of ≥ 6 mice per group. *, $p < 0.05$; **, $p < 0.01$; anti-S100 protein vs control IgG groups, Dunnett multiple comparison test.



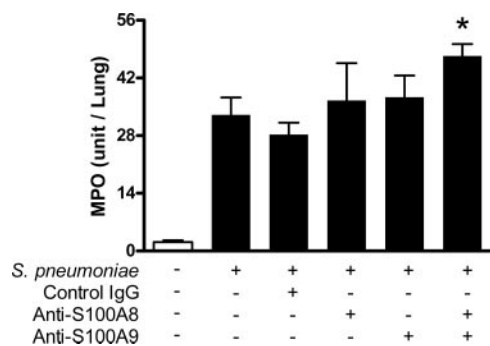


FIGURE 7. Effects of anti-S100A8 and anti-S100A9 on neutrophil recruitment into the lung 48 h postinfection. CD1 mice were injected i.p. with 2 mg of purified rabbit IgG against S100A8, and/or S100A9, or nonimmune serum 16 h before infection. The mice were then infected with *S. pneumoniae*. At 48 h postinfection, the lungs were homogenized, and endogenous myeloperoxidase was measured. Values represent the mean \pm SEM of ≥ 6 mice per group. *, $p < 0.05$, anti-S100 protein vs control IgG groups Dunnett multiple comparison test.

and anti-S100A9-treated mice. Moreover, no significant changes in the number of neutrophils sequestered in the lung vasculature were observed by blocking S100A8 and S100A9 proteins compared with control mice (Fig. 8B). In addition, the number of circulating neutrophils remained unaffected by the injection of anti-S100 proteins (data not shown).

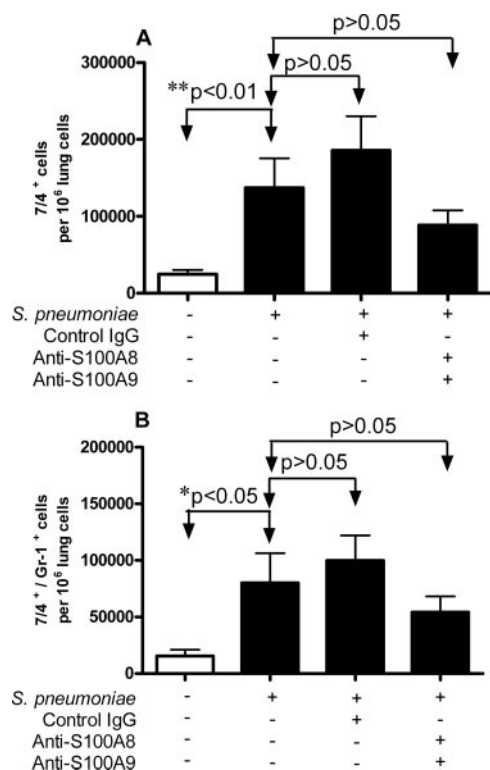


FIGURE 8. A and B, effects of S100A8 and S100A9 on neutrophil sequestration in the lung vasculature. CD1 mice were injected i.p. with 2 mg of purified rabbit IgG against S100A8 and S100A9, or nonimmune serum 16 h before infection with *S. pneumoniae*. At 48 h postinfection, 10 μ g of FITC-labeled anti-Gr-1 were injected i.v. and 10 min later lungs were harvested. Single-cell preparations of lungs were stained with anti-7/4 to identify the total neutrophil population in the lung. Gr-1⁺ cells represent the sequestered neutrophils in the lung. Values represent the mean \pm SEM of ≥ 6 mice per group. *, $p < 0.05$; **, $p < 0.01$; anti-S100 protein vs control IgG groups, Dunnett multiple comparison test.

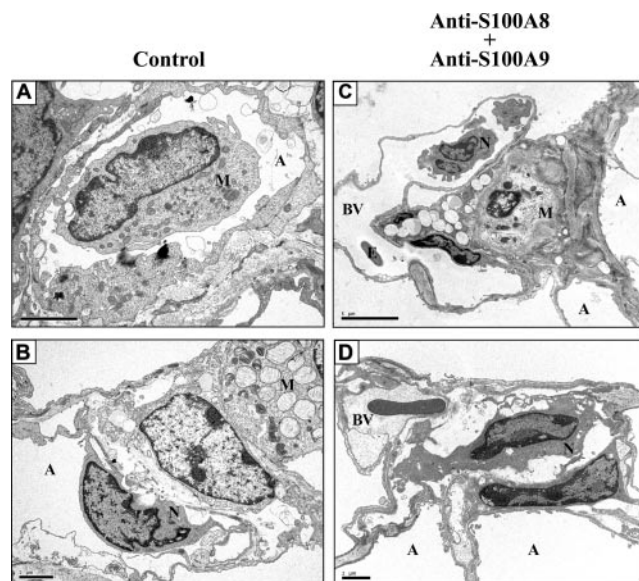


FIGURE 9. Electron microscopy analyses of the effects of anti-S100A8 and anti-S100A9 on neutrophil recruitment into the lung 48h postinfection. CD1 mice were injected i.p. with 2 mg of purified rabbit IgG against S100A8, and/or S100A9, or nonimmune serum 16 h before infection. The mice were then infected with *S. pneumoniae*. At 48 h postinfection, the lungs were fixed and processed for electron microscopy. A and B, macrophage and neutrophils in alveoli of control animals; C and D, macrophages and neutrophils in lung tissue of anti-S100A8 and anti-S100A9-treated animals. A, alveolar space; BV, blood vessel; M, macrophage; N, neutrophils.

Similarly, electron microscopy analyses of lung tissues show neutrophils and macrophages in alveoli of infected animals (Fig. 9, A and B), whereas most of the neutrophils and macrophages were found in lung tissue, but not alveoli of anti-S100A8 and anti-S100A9-treated animals (Fig. 9, C and D). These results confirmed the hypothesis that S100A8 and S100A9 are important for neutrophil transepithelial, but not transendothelial migration in the lung.

To further decipher the mechanism by which anti-S100A8 and anti-S100A9 caused the accumulation of phagocytes in lung tissue, the expression of the chemokines CXCL1, CXCL2, and CCL2 was evaluated by ELISA in BAL and lung tissues. Treatment of mice with anti-S100A9 alone or in combination with anti-S100A8 led to 50 and 100% increases in the lungs of CCL2 and CXCL2 levels, respectively, compared with control mice. (Fig. 10, A, C, and E; $p < 0.01$ for CXCL2 and $p < 0.05$ for CCL2, Dunnett multiple comparison test). However, a 2.5-fold increase of CCL2 levels was also observed in the BAL of mice treated with anti-S100A9 or anti-S100A9 in combination with S100A8. (Fig. 10, B, D, and F; $p < 0.01$, Dunnett multiple comparison test). Similarly, a 20% increase of CXCL1 levels was observed after the blockade of S100A8 and S100A9. The augmented presence of chemokines attracting both neutrophils and monocyte/macrophages in the BAL and lung tissues of anti-S100A8 and anti-S100A9-treated mice was convincing evidence against an indirect effect of S100A8 and S100A9 in directing phagocyte migration in the lung.

Discussion

In this study, we examined the functions of S100A8 and S100A9 by observing leukocyte migration in the mouse lung during streptococcal pneumonia. Our results indicate that S100A8 and S100A9 are released differentially during the course of infection. At an early phase of infection, the pneumocytes might be one of the sources of these two proteins. This presence is correlated with

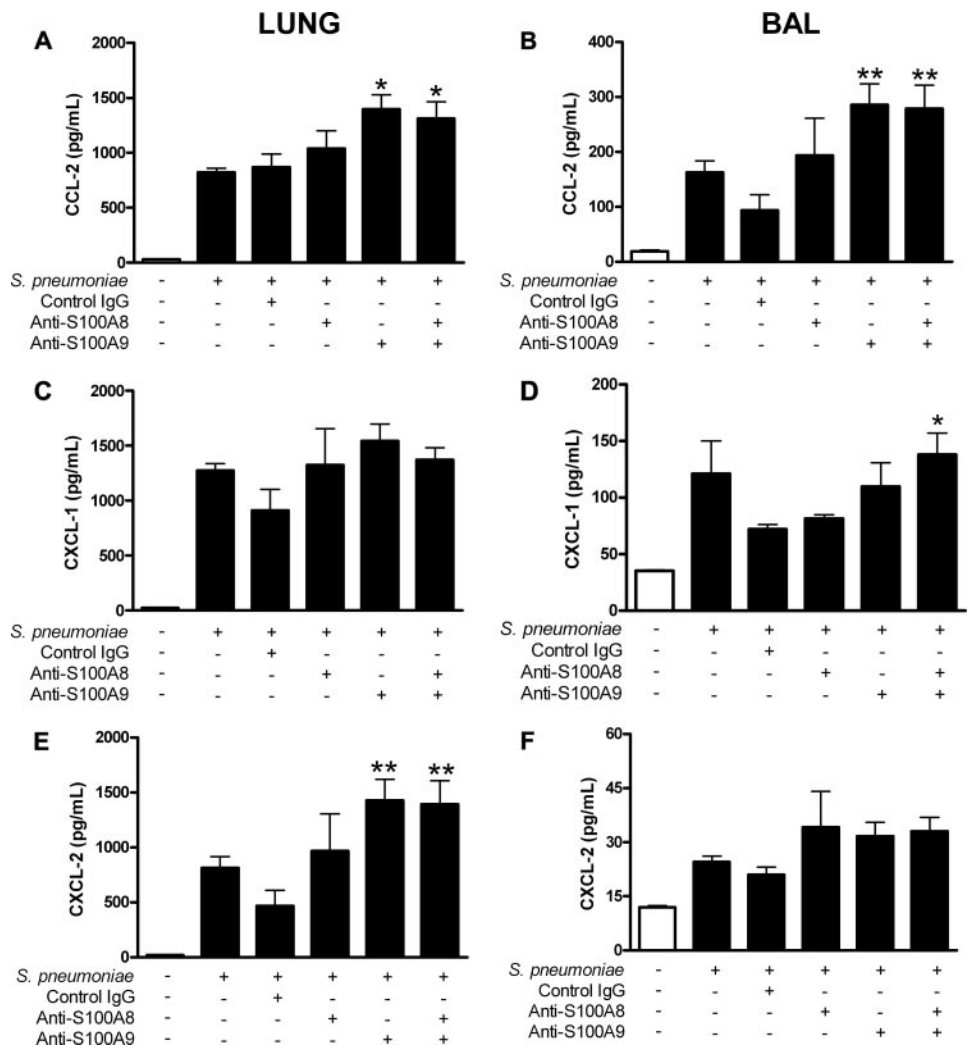


FIGURE 10. Effects of S100A8 and S100A9 on levels of CCL2, CXCL1, and CXCL2 in BAL and lung 48 h postinfection. CD1 mice were injected i.p. with 2 mg of purified rabbit IgG against S100A8 and/or S100A9, or nonimmune serum 16 h before infection. Mice were then infected with *S. pneumoniae*. At 48 h postinfection, BAL and lung were harvested, and the quantities of CCL-2, CXCL1, and CXCL2 were measured in the lung homogenates (A, C, and E) and BAL (B, D, and F). Values represent the mean \pm SEM of ≥ 6 mice per group. *, $p < 0.05$; **, $p < 0.01$; anti-S100 protein vs control IgG groups, Dunnett multiple comparison test.

increased neutrophil and macrophage migration at latter stages of infection. More importantly, blockade of S100A8 and S100A9 activity strongly inhibited phagocyte recruitment to the alveoli without affecting the sequestration of neutrophils within the vasculature, or the number of circulating neutrophils or their migration in lung tissue. The reduced migration of phagocytes in the alveoli was not caused by altered secretion of chemokines in the lung tissue or alveoli. What emerges from the results is the importance of these antimicrobial proteins in promoting leukocyte migration to the lung alveoli.

A possible explanation for these observations would be that S100A8 and S100A9 act by preventing neutrophil apoptosis. The observed reduced numbers of neutrophils in the alveolar space could therefore be explained by an enhanced apoptosis of neutrophils in the presence of anti-S100A8 and anti-S100A9. However, this is unlikely to be the case as a similar diminution of neutrophils numbers in Ab-treated animals was not seen in lung tissue. In addition, we observed very few apoptosing neutrophils in BALs of untreated or Ab-treated animals, either by flow cytometry, optical or electron microscopy.

S100A8 and S100A9 did not induce the transepithelial migration of phagocytes indirectly by inducing the secretion of chemokines in the alveolar lumen, given that alveolar secretion of CXCL1 and CCL2 was down-regulated by S100A8 and S100A9. This is intriguing considering that S100A8 and S100A9 induce the expression and secretion of CXCL8 in epithelial cells (35) and of

proinflammatory cytokines such as IL-6, CXCL8, IL-1 β , and TNF- α in monocytes (36). The increased presence of chemokines in the BAL of anti-S100A8- and anti-S100A9-treated animals was associated with a diminished presence of phagocytes. It is thus possible that the reduced uptake of chemokines via chemokine receptors present on (fewer) leukocytes could contribute to this augmentation, although the increased presence of chemokines and phagocytes (as observed by myeloperoxidase) in lung tissue provide evidence against this hypothesis. Alternatively, the secretion of an inhibitory molecule by phagocytes that down-regulates the secretion of CCL2 and CXCL1 could also explain this effect. Further experimentation will be necessary to test these hypotheses.

Antimicrobial peptides and chemokines are simultaneously present in the lung during streptococcal infection and the task of distinguishing their relative functions is complex. Recently, studies have shown that antimicrobial and chemotactic peptides have certain activities in common; for example, defensins and CAP37, both antimicrobial peptides, induce weak to moderate inflammatory reaction when injected in mice (3). Moreover, β -defensins bind and activate the chemokine receptor CCR6 (37). Conversely, antimicrobial activities have been attributed to certain chemokines (1, 2). These duplicated activities make it difficult to ascertain the relative roles of these cytokines. Studies by Fillion and others, using a combination of three neutralizing Abs (anti-CCL2, anti-CCL3, and anti-CCL5) in *S. pneumoniae*-infected mice showed

only a 33% reduction in macrophage infiltration and no significant decrease in neutrophil migration in the alveolar space (38). Similarly, blockade of CXCL2 activities led to only a 20% decrease of neutrophil recruitment in the airspace in a pneumolysin-induced lung inflammation (39). These results suggest that these chemokines could have a relatively minor role in neutrophil migration to the lung during streptococcal infection. This is in contrast to the drastic effect of inhibition of S100A8 and S100A9, which emphasizes the importance of these proteins in the innate response.

The various chemotactic signals present at the inflammatory site probably act in sequence (40), and some chemotactic factors probably stimulate leukocyte firm adhesion to the endothelium to promote transendothelial migration. Other chemotactic factors then guide leukocytes within the tissue to the general area of inflammation where pathogen- and innate immunity-derived factors (such as formyl peptides and C5a) override these signals and lead phagocytes to the pathogen. The importance of this sequential action of chemotactic factors emerged in a study by Coates and McColl (41), who showed that the activities of complement-derived factors dominate over chemokines during leukocyte migration in response to bacterial infection. That inhibition of S100A8 and S100A9 blocks phagocyte migration to the alveoli, but not lung tissue, and supports that these proteins play a role in the last steps of phagocyte migration.

Leukocyte migration to the lung is tightly regulated. To gain access to the luminal space, leukocytes must first extravasate, migrate within the lung tissue, and then cross the basolateral to the luminal side of the epithelial cells. S100A9 and S100A8/A9 were previously shown to promote monocyte transendothelial migration (42). In addition, S100A9 stimulates neutrophil adhesion to the extracellular matrix protein fibronectin (N. Anceriz and P. A. Tessier, unpublished observations). Thus, the assumption that S100A9 could facilitate leukocyte extravasation and movement within the tissue is valid; however, in our experiments phagocytes accumulated within the tissue in mice treated with anti-S100A8 and anti-S100A9, which favors that S100A8 and S100A9 play important roles in neutrophil migration across epithelial cells, but not in lung transendothelial migration. This is intriguing as it implies a specialized role for S100A8 and S100A9 in transepithelial migration. Interestingly, such an activity has been recently described for heparanase, a lipid mediator (43).

S100A8 and S100A9 regulate the passage of leukocytes through the endothelium by enhancing the expression of adhesion molecules such as ICAM-1 and VCAM-1 on endothelial cells (44) and by activating their counterreceptor Mac-1 on neutrophils (26, 45). In addition, S100A8/A9 has recently been shown to down-regulate tight junction proteins on endothelial cells (44). Thus, they could facilitate leukocyte transendothelial migration by enhancing both leukocyte adhesion and endothelial cell permeability. Although S100A8 and S100A9 are not critical to neutrophil transendothelial migration in the lung, they could play a similar role by increasing the permeability of the alveolar epithelium by regulating tight junction genes. Additional experiments are needed to test this hypothesis.

It is becoming increasingly clear that the release of intracellular contents of any cell into the extracellular space activates the immune system. As the first cells to reach inflammatory sites, neutrophils are well positioned to signal impending harm. S100A8/A9 accounts for almost 40% of neutrophil cytosolic proteins (46). In addition, S100A8 and S100A9 induce NF κ B activation in mononuclear cells, activate lymphocyte, and assist neutrophil and monocyte migration (27, 36, 42, 47). As such, they are powerful danger signals that activate both the innate and adaptive immune re-

sponses. Consequently, the death of few cells, particularly neutrophils, or the active secretion of their intracellular content, could send a powerful danger signal alerting the innate immune system of damage caused by a pathogen. That S100A8 was more important in neutrophil migration to the lung in response to *S. pneumoniae* infection than LPS-induced inflammation (48) supports this idea. This might reflect a role for S100A8 and S100A9 as danger signals for the immune system, as unlike a true bacterial infection, LPS inflammation would not result in the death of cells.

In conclusion, in these murine studies, we report convincing evidence of the critical role of S100A8 and S100A9 proteins of regulating macrophage and neutrophil transepithelial migration from the lung tissue to the alveolar space in the host response to *S. pneumoniae* infection. These results indicate the importance of antimicrobial peptides, as opposed to classic chemotactic factors, in regulating inflammatory reactions. In addition, they suggest that S100 proteins could act as potent danger signals for the immune system.

Acknowledgments

We thank Susanne Richardson for reviewing this manuscript and the technicians from the Université Laval electron microscopy service for their help in preparation and analysis of lung sections.

Disclosures

The authors have no financial conflict of interest.

References

- Yang, D., Q. Chen, D. M. Hoover, P. Staley, K. D. Tucker, J. Lubkowski, and J. J. Oppenheim. 2003. Many chemokines including CCL20/MIP-3 α display antimicrobial activity. *J. Leukocyte Biol.* 74: 448–455.
- Cole, A. M., T. Ganz, A. M. Liese, M. D. Burdick, L. Liu, and R. M. Strieter. 2001. Cutting edge: IFN-inducible ELR-CXC chemokines display defensin-like antimicrobial activity. *J. Immunol.* 167: 623–627.
- Chertov, O., D. F. Michiel, L. Xu, J. M. Wang, K. Tani, W. J. Murphy, D. L. Longo, D. D. Taub, and J. J. Oppenheim. 1996. Identification of defensin-1, defensin-2, and CAP37/azurocidin as T-cell chemoattractant proteins released from interleukin-8-stimulated neutrophils. *J. Biol. Chem.* 271: 2935–2940.
- Chertov, O., H. Ueda, L. L. Xu, K. Tani, W. J. Murphy, J. M. Wang, O. M. Howard, T. J. Sayers, and J. J. Oppenheim. 1997. Identification of human neutrophil-derived cathepsin G and azurocidin/CAP37 as chemoattractants for mononuclear cells and neutrophils. *J. Exp. Med.* 186: 739–747.
- Territo, M. C., T. Ganz, M. E. Selsted, and R. Lehrer. 1989. Monocyte-chemotactic activity of defensins from human neutrophils. *J. Clin. Invest.* 84: 2017–2020.
- Striz, I., and I. Trebichavsky. 2004. Calprotectin: a pleiotropic molecule in acute and chronic inflammation. *Physiol. Res.* 53: 245–253.
- Barthe, C., C. Figarella, J. Carrere, and O. Guy-Crotte. 1991. Identification of “cystic fibrosis protein” as a complex of two calcium-binding proteins present in human cells of myeloid origin. *Biochim. Biophys. Acta* 1096: 175–177.
- Berntzen, H. B., U. Olmez, M. K. Fagerhol, and E. Munthe. 1991. The leukocyte protein L1 in plasma and synovial fluid from patients with rheumatoid arthritis and osteoarthritis. *Scand. J. Rheumatol.* 20: 74–82.
- Hu, S. P., C. Harrison, K. Xu, C. J. Cornish, and C. L. Geczy. 1996. Induction of the chemotactic S100 protein, CP-10, in monocyte/macrophages by lipopolysaccharide. *Blood* 87: 3919–3928.
- Lusitani, D., S. E. Malawista, and R. R. Montgomery. 2003. Calprotectin, an abundant cytosolic protein from human polymorphonuclear leukocytes, inhibits the growth of *Borrelia burgdorferi*. *Infect. Immun.* 71: 4711–4716.
- Nisapakultorn, K., K. F. Ross, and M. C. Herzberg. 2001. Calprotectin expression inhibits bacterial binding to mucosal epithelial cells. *Infect. Immun.* 69: 3692–3696.
- Santhanagopalan, V., B. L. Hahn, B. E. Dunn, J. H. Weissner, and P. G. Sohnle. 1995. Antimicrobial activity of calprotectin isolated from human empyema fluid supernatants. *Clin. Immunol. Immunopathol.* 76: 285–290.
- Brandtzaeg, P., T. O. Gabrielsen, I. Dale, F. Muller, M. Steinbakk, and M. K. Fagerhol. 1995. The leukocyte protein L1 (calprotectin): a putative non-specific defence factor at epithelial surfaces. *Adv. Exp. Med. Biol.* 371A: 201–206.
- Clohesy, P. A., and B. E. Golden. 1995. Calprotectin-mediated zinc chelation as a biostatic mechanism in host defence. *Scand. J. Immunol.* 42: 551–556.
- Clohesy, P. A., and B. E. Golden. 1996. The mechanism of calprotectin's candidastatic activity appears to involve zinc chelation. *Biochem. Soc. Trans.* 24: 309S.
- Miyasaka, K. T., A. L. Bodeau, A. R. Murthy, and R. I. Lehrer. 1993. In vitro antimicrobial activity of the human neutrophil cytosolic S-100 protein complex, calprotectin, against *Capnocytophaga sputigena*. *J. Dent. Res.* 72: 517–523.

17. Murthy, A. R., R. I. Lehrer, S. S. Harwig, and K. T. Miyasaki. 1993. In vitro candidastatic properties of the human neutrophil calprotectin complex. *J. Immunol.* 151: 6291–6301.
18. Nisapakultorn, K., K. F. Ross, and M. C. Herzberg. 2001. Calprotectin expression in vitro by oral epithelial cells confers resistance to infection by *Porphyromonas gingivalis*. *Infect. Immun.* 69: 4242–4247.
19. Sohnle, P. G., C. Collins-Lech, and J. H. Wiessner. 1991. The zinc-reversible antimicrobial activity of neutrophil lysates and abscess fluid supernatants. *J. Infect. Dis.* 164: 137–142.
20. Sohnle, P. G., M. J. Hunter, B. Hahn, and W. J. Chazin. 2000. Zinc-reversible antimicrobial activity of recombinant calprotectin (migration inhibitory factor-related proteins 8 and 14). *J. Infect. Dis.* 182: 1272–1275.
21. Berntzen, H. B., E. Munthe, and M. K. Fagerhol. 1989. A longitudinal study of the leukocyte protein L1 as an indicator of disease activity in patients with rheumatoid arthritis. *J. Rheumatol.* 16: 1416–1420.
22. Frosch, M., A. Strey, T. Vogl, N. M. Wulffraat, W. Kuis, C. Sunderkotter, E. Harms, C. Sorg, and J. Roth. 2000. Myeloid-related proteins 8 and 14 are specifically secreted during interaction of phagocytes and activated endothelium and are useful markers for monitoring disease activity in pauciarticular-onset juvenile rheumatoid arthritis. *Arthritis Rheum.* 43: 628–637.
23. Ryckman, C., C. Gilbert, R. de Medicis, A. Lussier, K. Vandal, and P. A. Tessier. 2004. Monosodium urate monohydrate crystals induce the release of the proinflammatory protein S100A8/A9 from neutrophils. *J. Leukocyte Biol.* 76: 433–440.
24. Odink, K., N. Cerletti, J. Bruggen, R. G. Clerc, L. Tarcsay, G. Zwadlo, G. Gerhards, R. Schlegel, and C. Sorg. 1987. Two calcium-binding proteins in infiltrate macrophages of rheumatoid arthritis. *Nature* 330: 80–82.
25. Youssef, P., J. Roth, M. Frosch, P. Costello, O. Fitzgerald, C. Sorg, and B. Bresnahan. 1999. Expression of myeloid related proteins (MRP) 8 and 14 and the MRP8/14 heterodimer in rheumatoid arthritis synovial membrane. *J. Rheumatol.* 26: 2523–2528.
26. Ryckman, C., K. Vandal, P. Rouleau, M. Talbot, and P. A. Tessier. 2003. Proinflammatory activities of S100: proteins S100A8, S100A9, and S100A8/A9 induce neutrophil chemotaxis and adhesion. *J. Immunol.* 170: 3233–3242.
27. Vandal, K., P. Rouleau, A. Boivin, C. Ryckman, M. Talbot, and P. A. Tessier. 2003. Blockade of S100A8 and S100A9 suppresses neutrophil migration in response to lipopolysaccharide. *J. Immunol.* 171: 2602–2609.
28. Cornish, C. J., J. M. Devery, P. Poronnik, M. Lackmann, D. I. Cook, and C. L. Geczy. 1996. S100 protein CP-10 stimulates myeloid cell chemotaxis without activation. *J. Cell. Physiol.* 166: 427–437.
29. Ryckman, C., S. R. McColl, K. Vandal, R. de Medicis, A. Lussier, P. E. Poubelle, and P. A. Tessier. 2003. Role of S100A8 and S100A9 in neutrophil recruitment in response to monosodium urate monohydrate crystals in the air-pouch model of acute gouty arthritis. *Arthritis Rheum.* 48: 2310–2320.
30. Kadioglu, A., and P. W. Andrew. 2004. The innate immune response to pneumococcal lung infection: the untold story. *Trends Immunol.* 25: 143–149.
31. Bergeron, Y., N. Ouellet, A. M. Deslauriers, M. Simard, M. Olivier, and M. G. Bergeron. 1998. Cytokine kinetics and other host factors in response to pneumococcal pulmonary infection in mice. *Infect. Immun.* 66: 912–922.
32. Reutershan, J., A. Basit, E. V. Galkina, and K. Ley. 2005. Sequential recruitment of neutrophils into lung and bronchoalveolar lavage fluid in LPS-induced acute lung injury. *Am. J. Physiol.* 289: L807–L815.
33. Passey, R. J., E. Williams, A. M. Lichanska, C. Wells, S. Hu, C. L. Geczy, M. H. Little, and D. A. Hume. 1999. A null mutation in the inflammation-associated S100 protein S100A8 causes early resorption of the mouse embryo. *J. Immunol.* 163: 2209–2216.
34. Ramisse, F., P. Binder, M. Szatanik, and J. M. Alonso. 1996. Passive and active immunotherapy for experimental pneumococcal pneumonia by polyvalent human immunoglobulin or F(ab')₂ fragments administered intranasally. *J. Infect. Dis.* 173: 1123–1128.
35. Ahmad, A., D. L. Bayley, S. He, and R. A. Stockley. 2003. Myeloid related protein-8/14 stimulates interleukin-8 production in airway epithelial cells. *Am. J. Respir. Cell Mol. Biol.* 29: 523–530.
36. Sunahori, K., M. Yamamura, J. Yamana, K. Takasugi, M. Kawashima, H. Yamamoto, W. J. Chazin, Y. Nakatani, S. Yui, and H. Makino. 2006. The S100A8/A9 heterodimer amplifies proinflammatory cytokine production by macrophages via activation of nuclear factor κ B and p38 mitogen-activated protein kinase in rheumatoid arthritis. *Arthritis Res Ther.* 8: R69.
37. Yang, D., O. Chertov, S. N. Bykovskaia, Q. Chen, M. J. Buffo, J. Shogan, M. Anderson, J. M. Schroder, J. M. Wang, O. M. Howard, and J. J. Oppenheim. 1999. β -Defensins: linking innate and adaptive immunity through dendritic and T cell CCR6. *Science* 286: 525–528.
38. Fillion, I., N. Ouellet, M. Simard, Y. Bergeron, S. Sato, and M. G. Bergeron. 2001. Role of chemokines and formyl peptides in pneumococcal pneumonia-induced monocyte/macrophage recruitment. *J. Immunol.* 166: 7353–7361.
39. Rijneveld, A. W., G. P. van den Dobbela, S. Florquin, T. J. Standiford, P. Speelman, L. van Alphen, and T. van der Poll. 2002. Roles of interleukin-6 and macrophage inflammatory protein-2 in pneumolysin-induced lung inflammation in mice. *J. Infect. Dis.* 185: 123–126.
40. Heit, B., S. Tavener, E. Raharjo, and P. Kubes. 2002. An intracellular signaling hierarchy determines direction of migration in opposing chemotactic gradients. *J. Cell Biol.* 159: 91–102.
41. Coates, N. J., and S. R. McColl. 2001. Production of chemokines in vivo in response to microbial stimulation. *J. Immunol.* 166: 5176–5182.
42. Eue, I., B. Pietz, J. Storck, M. Klempt, and C. Sorg. 2000. Transendothelial migration of 27E10⁺ human monocytes. *Int. Immunol.* 12: 1593–1604.
43. Hurley, B. P., D. Siccardi, R. J. Mrsny, and B. A. McCormick. 2004. Polymorphonuclear cell transmigration induced by *Pseudomonas aeruginosa* requires the eicosanoid heptaxilin A3. *J. Immunol.* 173: 5712–5720.
44. Viemann, D., A. Strey, A. Janning, K. Jurk, K. Klimmek, T. Vogl, K. Hirono, F. Ichida, D. Foell, B. Kehrel, et al. 2005. Myeloid-related proteins 8 and 14 induce a specific inflammatory response in human microvascular endothelial cells. *Blood* 105: 2955–2962.
45. Newton, R. A., and N. Hogg. 1998. The human S100 protein MRP-14 is a novel activator of the β_2 integrin Mac-1 on neutrophils. *J. Immunol.* 160: 1427–1435.
46. Edgeworth, J., M. Gorman, R. Bennett, P. Freemont, and N. Hogg. 1991. Identification of p8,14 as a highly abundant heterodimeric calcium binding protein complex of myeloid cells. *J. Biol. Chem.* 266: 7706–7713.
47. Ryckman, C., G. A. Robichaud, J. Roy, R. Cantin, M. J. Tremblay, and P. A. Tessier. 2002. HIV-1 transcription and virus production are both accentuated by the proinflammatory myeloid-related proteins in human CD4⁺ T lymphocytes. *J. Immunol.* 169: 3307–3313.
48. Bozinovski, S., M. Cross, R. Vlahos, J. E. Jones, K. Hsu, P. A. Tessier, E. C. Reynolds, D. A. Hume, J. A. Hamilton, C. L. Geczy, and G. P. Anderson. 2005. S100A8 chemotactic protein is abundantly increased, but only a minor contributor to LPS-induced, steroid resistant neutrophilic lung inflammation in vivo. *J. Proteome Res.* 4: 136–145.